

# Low-redshift tests of cosmologies with a time-varying gravitational constant

Ekim Taylan Hanimeli,<sup>a,b,1</sup> Isaac Tutusaus,<sup>c,d,a</sup> Brahim Lamine,<sup>a</sup>  
Alain Blanchard<sup>a</sup>

<sup>a</sup>Université de Toulouse, UPS-OMP, IRAP, CNRS, 14 Avenue Edouard Belin, F-31400 Toulouse, France

<sup>b</sup>Luleå University of Technology, Space Campus, Rymd-campus 1, 981 92 Kiruna, Sweden

<sup>c</sup>Institute of Space Sciences (ICE, CSIC), Campus UAB, Carrer de Can Magrans, s/n, 08193 Barcelona, Spain

<sup>d</sup>Institut d'Estudis Espacials de Catalunya (IEEC), Carrer Gran Capità 2-4, 08193 Barcelona, Spain

E-mail: [ekimtaylan@gmail.com](mailto:ekimtaylan@gmail.com), [tutusaus@ice.csic.es](mailto:tutusaus@ice.csic.es),  
[Brahim.Lamine@irap.omp.eu](mailto:Brahim.Lamine@irap.omp.eu), [alain.blanchard@irap.omp.eu](mailto:alain.blanchard@irap.omp.eu)

**Abstract.** In this work we investigate cosmologies with a time-varying gravitational constant,  $G(t)$ , as an alternative to having a cosmological constant. Since, it is known in the literature that, in general relativity, having a variable gravitational constant breaks the conservation of energy unless further dynamical components are added, we consider a Newtonian approach, in which the energy conservation is ensured. We investigate whether these cosmologies are able to reproduce the cosmological acceleration without a cosmological constant, nor any other sort of dark energy fluid. After constructing the Friedmann-Lemaître equation for a late-stage, matter dominated universe by starting with Newton's second law, where  $G$  is taken as a function of time, we create specific models to test against cosmological observations. In this Friedmann-Lemaître equation we obtain a second gravitational constant,  $G^*$ , related to the original  $G$  in the acceleration equation. For the tests we focus on the acceleration period and use low-redshift probes: type Ia supernovae (SNIa), baryon acoustic oscillations, and cosmic chronometers, taking also into account a possible change in the supernova intrinsic luminosity with redshift. As a result, we obtain several models without a cosmological constant with similar or even slightly better  $\chi^2$  values than the standard  $\Lambda$ CDM cosmology. When SNIa luminosity dependence on redshift is added, a model with a  $G$  exponentially decreasing to zero today can explain the observations. In the cases where SNIa are assumed to be standard candles, the observations favour a negative  $G$  at large scales to produce cosmic acceleration. We conclude that these models offer a viable interpretation of the late-time universe observations.

---

<sup>1</sup>Corresponding author.

---

## Contents

<b>1</b>	<b>Introduction</b>	<b>1</b>
<b>2</b>	<b>Construction of the models</b>	<b>3</b>
<b>3</b>	<b>Data and methodology</b>	<b>4</b>
3.1	Type Ia supernovae	4
3.2	Baryon acoustic oscillations	5
3.3	Direct $H(z)$ measurements	6
3.4	Determination of the parameter constraints	6
<b>4</b>	<b>Results and discussion</b>	<b>7</b>
<b>5</b>	<b>Conclusion</b>	<b>12</b>

---

## 1 Introduction

The accelerating expansion of the universe [1, 2] is a widely accepted idea with a large amount of observational support (see e.g. the reviews [3, 4] and references therein). In the standard model of cosmology,  $\Lambda$ CDM, this acceleration is interpreted as a cosmological constant,  $\Lambda$ , which acts as the vacuum energy with positive energy density but negative pressure. However, the value of this constant is at odds with quantum field theoretical estimations of the vacuum energy, which creates the cosmological constant problem [5]. Moreover, on the observational side, there has recently been a debate in the literature about whether SNIa data (either alone or combined with other probes) can definitely prove the accelerated nature of the expansion of the Universe [6–17]. Therefore, it is reasonable to question this standard cosmological picture from both theoretical and observational perspectives.

In this work, we focus on cosmologies where the gravitational constant,  $G$ , varies in time, as an alternative to cosmologies with a cosmological constant. Having a time-varying gravitational constant is an old idea, dating back at least to Dirac and his large numbers hypothesis [18]. Accordingly, in the literature there are multiple ways of implementing such a variation. One popular way is to replace the gravitational constant with a dynamical scalar field evolving with time (and space). The most interesting feature of such scenarios is that the theory is then fully compatible with Mach’s principle, giving a physical explanation to inertia. The most extensively studied relativistic models among these are the so-called Jordan-Brans-Dicke (JBD) theories [19, 20]. These theories, and some of their extensions, have been confronted with observations for many decades, and very tight constraints have been put on them with solar system measurements. In particular, the original JBD model introduces a dimensionless parameter  $\omega$ , which should naturally be of order unity, but is constrained to be larger than roughly 50 000 by solar system tests [21]. In order to overcome these solar system constraints, screening mechanisms can be added to these theories to separate their predictions in cosmological scales from the local observations (for a more detailed discussion of various screening mechanisms see [22]). Similarly, in this analysis we also assume that our model is only valid at the cosmological scales, but not at small scales. We justify this

assumption by the possible existence of a screening mechanism applicable in our case, but we will not attempt to detail this mechanism, as it is outside the scope of this text.

Another possibility for implementing a time-varying  $G$  is to consider the phenomenology of a variable gravitational constant directly in Einstein’s equations. However, it is well known that the geometry of general relativity puts restrictions on the contents of the universe due to Bianchi identities, and these restrictions may break the usual conservation of energy in the case of a variable  $G$  [23]. For this reason, it is suggested [24] that a Newtonian approach may be more suitable for considering cosmologies with variable  $G$ , if adding other constituents to the universe in place of the gravitational constant is not desired. Newtonian cosmologies with varying  $G$  have previously been investigated [25] and, in spirit, could be considered similar to MOND theories [26], which propose modifications to Newtonian dynamics in order to explain galaxy observations without dark matter. Various other aspects of Newtonian  $G(t)$  dynamics have also been studied in the literature [27, 28]. Following these, in the present paper we adopt a modified Newtonian approach instead of a relativistic one, while a general relativistic treatment will be carried out in a later work. The goal of this analysis is to know whether a modified Newtonian model with a varying  $G$  and without a cosmological constant or any kind of dark energy can fit the low redshift probes in a comparable way to  $\Lambda$ CDM.

In a similar way to an earlier analysis [25], our starting point is a modified Newton’s second law, where we take Newton’s gravitational constant to be any well-behaved function of time (or equivalently of the scale factor  $a$ ). We then continue by deriving the analogues of Friedmann-Lemaître equations. Once the main cosmological equations are obtained, we specify the  $G(t)$  models to test. We consider two different functions, an exponential and a power series  $G(t)$ . We envision the latter as an expansion of some general function, centered around the present epoch since we want to focus on the late stages where the acceleration is relevant. This allows us to see the general late stage behaviour of  $G$  required in order to replace the cosmological constant. For the exponential function we try two different versions with positive and negative parameters. The model with positive parameter is intended to interpolate to a non-accelerating model today, such as the  $R_h = ct$  cosmology [29, 30] (see also [31, 32] and references therein for analyses with this kind of models), while the model with negative parameter achieves a negative  $G$  at the late stage as an alternative to a negative pressure ( $w = -1$ ) in the standard cosmological picture while remaining approximately constant in the early Universe.

As said before, in this work we focus on the low-redshift range, where a cosmological constant is relevant, leaving a possible generalization to the early Universe for future work. Accordingly, we compare the predictions of our models to low-redshift probes: type Ia supernovae, baryon acoustic oscillations, and  $H(z)$  measurements. Even though our screening assumption might, in principle, imply that SNIa will not be affected by a varying  $G$ , some influence is still possible, for example, due to imperfect screening inside dense matter (see for example Koyama et al. [33] for an imperfect Vainshtein mechanism inside stars). Moreover, there may be other justifications for adding a redshift dependence to the supernovae (see Tutusaus et al. [11] and references therein for previous analyses considering this redshift dependence). We account for these possibilities by allowing SNIa intrinsic luminosity to depend on redshift.

This paper is organized as follows: in Section 2 we present the derivation of our cosmological models for varying  $G$  functions using a Newtonian approach. In Section 3 we describe the different cosmological probes and data sets used in this analysis, as well as the methodology adopted to fit the models to the data. The main results of this work are presented in

Section 4, and we conclude in Section 5.

## 2 Construction of the models

We start by envisioning Newton's second law being applied to a uniform, dust sphere of radius  $R$  and mass  $M = 4\pi R^3 \rho / 3$ , with  $\rho$  being the mass density

$$-\frac{GM}{R^2} = \ddot{R}, \quad (2.1)$$

where the dots represent the derivative with respect to the time coordinate. We assume the Universe to be isotropic and homogeneous, and therefore this equation could be written centered at any point.

Let us now assume that Newton's gravitational constant depends on time,  $G = G(t)$ , or equivalently on  $R$ . An integration with respect to  $R$  gives an energy relation,

$$M \left[ \frac{G}{R} - \int \frac{dG}{R} \right] = \frac{1}{2} \dot{R}^2 - C, \quad (2.2)$$

where  $C$  is an integration constant (related in general relativity to spatial curvature [34]). We can then obtain from the previous relation the modified Friedmann-Lemaître equation,

$$H^2 \equiv \frac{\dot{R}^2}{R^2} = \frac{8\pi}{3} \rho \left[ G - R \int \frac{dG}{R} \right] + \frac{2C}{R^2}. \quad (2.3)$$

For simplicity, we can redefine the term inside the parentheses as another gravitational parameter,  $G^*$ ,

$$G^* \equiv G - R \int \frac{dG}{R}. \quad (2.4)$$

With this definition, we essentially have two different gravitational parameters one,  $G$ , in Eq. 2.1 and another,  $G^*$ , in Eq. 2.3. Defining now the scale factor  $a = R/R_0$ , with  $R_0$  the current value of  $R$ , one has the following Friedmann-Lemaître equations

$$\ddot{a} = -\frac{4\pi}{3} G \rho, \quad H^2 = \frac{8\pi}{3} G^* \rho + \frac{kc^2}{a^2}, \quad (2.5)$$

with  $k = 2C/(R_0^2 c^2)$ . It is also convenient to define a critical energy density

$$\rho_c \equiv \frac{3H_0^2}{8\pi G_0^*}, \quad (2.6)$$

with  $G_0^* = G^*(z = 0)$ . We also introduce a density parameter  $\Omega = \rho/\rho_c$ . Because of mass conservation, we have  $R^3 \rho = \text{cst.}$ , or  $\rho = \rho_0/a^3 = \rho_0(1+z)^3$ , with  $z$  being the redshift. Replacing these in Eq. (2.3) we obtain the final form of the modified Friedmann-Lemaître equation used in this work

$$\frac{H^2(z)}{H_0^2} = \frac{G^*(z)}{G_0^*} \Omega (1+z)^3 + (1-\Omega)(1+z)^2. \quad (2.7)$$

The standard model is recovered if  $G(z)$  is constant and  $\Omega_\Lambda$  is added to this equation. We now consider two specific models for  $G(z)$  that are expressed, for convenience, as a function of the scale factor,  $a$ ,

$$(i) \quad G(a) = G_0(1 + \alpha_1(1-a) + \alpha_2(1-a)^2 + \dots) \quad (2.8)$$

$$(ii) \quad G(a) = G_\infty \left(1 + \frac{a}{\tilde{a}}\right) \exp\left(-\frac{a}{\tilde{a}}\right). \quad (2.9)$$

The first model is simply a Taylor expansion of  $G$  around the present ( $z = 0$ ). It introduces a few parameters,  $G_0$ ,  $\alpha_1$ ,  $\alpha_2$ , to be determined from the fit to observations. We stop the expansion at the second order since we have checked that going up to the third order does not help much in reducing the  $\chi^2$ , while we add unneeded extra parameters. Since  $G_0$  cancels out in Eq. (2.7), it is not constrained by the background cosmological probes.

The second model is an exponentially changing function, which we separate into two different scenarios to investigate them independently; one with  $\tilde{a}$  positive and another with  $\tilde{a}$  negative. In this model we have  $G^* = G_\infty \exp(-a/\tilde{a})$  for the second gravitational constant. As discussed in the introduction, the former is designed to approximate the  $R_h = ct$  cosmology while the latter is intended to consider the possibility of  $G$  exponentially dropping and changing sign at the late Universe.

As before,  $G_\infty$  is not determined by our calculations, since the cosmological probes used in this analysis are not sensitive to its absolute value. In this case,  $G_\infty$  is the value of  $G$  when  $z \rightarrow \infty$ . Since our investigation only concerns the low-redshift range, we can assume  $G_\infty$  to be the value of  $G$  at any higher redshift not covered by our analysis.

### 3 Data and methodology

In this section we describe the cosmological probes and the methodology used in this work. Starting with the former, we consider late-time cosmological probes to constrain the parameters of our cosmological models, namely type Ia supernovae, baryon acoustic oscillations, and direct measurements of the Hubble parameter,  $H(z)$ , from cosmic chronometers.

#### 3.1 Type Ia supernovae

For the treatment of SNIa data we use the measurements and covariance matrix provided by the joint light-curve analysis of Betoule et al. [35]. We obtain the observed distance modulus using the standardization method given by the authors,

$$\mu_{\text{obs}} = m - M + \alpha X - \beta C. \quad (3.1)$$

In this equation,  $m$ ,  $X$ , and  $C$  are the observed magnitude in the B-band rest frame, and the shape and colour standardization parameters for the different SNIa, respectively. These have been obtained in their analysis and provided in the public dataset. The remaining parameters,  $\alpha$ ,  $\beta$ , and  $M$  are nuisance parameters, common to all SNIa, that need to be determined together with the cosmological parameters from the fit to the data. The latter is the absolute magnitude in the B-band rest frame and, depending on the stellar mass of the host galaxy, it is given by an additional nuisance parameter  $\Delta M$ ,

$$M = \begin{cases} M', & \text{if } M_{\text{stellar}} < 10^{10} M_\odot \\ M' + \Delta M, & \text{otherwise,} \end{cases} \quad (3.2)$$

where  $M_{\text{stellar}}$  is the stellar mass of the host galaxy.

Additionally, we allow for the intrinsic luminosity of SNIa to change as a function of the redshift, as a consequence of an evolution of  $G$ , through an extra term in the standardization. This can be due to partial screening, as it is discussed before, or to some other unknown

mechanism. To take these possibilities into account, we add a phenomenological evolution, to the such that  $\mu_{\text{SNIa}} = \mu_{\text{obs}} - m_{\text{evo}}$  with,

$$m_{\text{evo}} = \epsilon z^\delta, \quad (3.3)$$

where  $\epsilon$  and  $\delta$  are nuisance parameters to be determined from the fit to the observations. In considering these two parameters, we leave  $\epsilon$  free, while we limited  $\delta$  to be non-zero and positive to avoid degeneracy between  $M$  and  $m_{\text{evo}}$  terms.

We compare the observed distance modulus to the predictions of the corresponding cosmological model using the definition

$$\mu = 5 \log_{10} (d_L H_0), \quad (3.4)$$

where the luminosity distance  $d_L$  is given by

$$d_L = (1+z)d_M = c(1+z) \int_0^z \frac{dz'}{H(z')}, \quad (3.5)$$

and  $d_M$  is the comoving distance for an expanding flat space, where flatness follows naturally from standard Newtonian mechanics.

### 3.2 Baryon acoustic oscillations

Baryon acoustic oscillations in the early universe create scales that are visible in the density distribution of galaxies. These scales can be measured using isotropic and anisotropic observations, and related back to cosmological quantities to constrain the parameters of a model. Isotropic observations measure the quantity  $D_V/r_d$ , with  $r_d$  being the length of the standard ruler and  $D_V$  given by

$$D_V(z) = \left( d_M^2(z) \frac{cz}{H(z)} \right)^{1/3}. \quad (3.6)$$

Anisotropic observations measure two quantities that relate to cosmological parameters, depending whether the observations are in the transverse or radial directions

$$\theta = \frac{r_d}{d_M}, \quad (3.7)$$

$$\delta z_s = \frac{r_d H(z)}{c}. \quad (3.8)$$

Let us mention that, while  $r_d$  is given by the comoving sound horizon at the end of the baryon drag epoch in the concordance model, it might have a different value for models differing from  $\Lambda$ CDM [36]. Therefore, in order to be as general as possible, and not delve into the physics of the early Universe, we consider  $r_d$  to be a free parameter in our analysis and let the data choose its preferred value.

In this analysis we consider the measurements from 6dFGS [37] at  $z = 0.106$ , SDSS-MGS [38] at  $z = 0.15$ , BOSS DR12 [39] at  $z = 0.38, 0.51, 0.61$ , and eBOSS DR14 [40] at  $z = 1.19, 1.50, 1.83$ , as well as the Ly- $\alpha$  auto-correlation function [41] and Ly- $\alpha$ -quasar cross correlation [42] at  $z = 2.4$ . We take into account the covariances for the BOSS and eBOSS measurements, we consider a correlation coefficient of  $-0.38$  for the Ly- $\alpha$  forest measurements, and we assume measurements of different surveys to be uncorrelated.

Due to the non-Gaussianity of the BAO observable likelihoods far from the peak, we replace the standard  $\Delta\chi_G^2 = -2\ln L_G$  for a Gaussian likelihood [43] by

$$\Delta\chi^2 = \frac{\Delta\chi_G^2}{\sqrt{1 + \Delta\chi_G^4 \left(\frac{S}{N}\right)^{-4}}}, \quad (3.9)$$

where  $S/N$  stands for the detection significance, in units of  $\sigma$ , of the BAO feature. We consider a detection significance of  $2.4\sigma$  for 6dFGS,  $2\sigma$  for SDSS-MGS,  $9\sigma$  for BOSS DR12,  $4\sigma$  for eBOSS DR14, and  $5\sigma$  for the Ly- $\alpha$  forest. Notice that some of these values are slightly lower than the ones quotes by the different collaborations in order to follow a conservative approach, and in case the likelihood becomes non-Gaussian at these high confidence levels.

### 3.3 Direct $H(z)$ measurements

Direct measurements of the Hubble parameter as a function of the redshift can be obtained with a relatively new method called cosmic chronometers [44]. This method employs observations of passive galaxies to determine their relative ages and redshifts. Since  $H(z) = -(dz/dt)/(1+z)$ , this method provides us with the information about recent expansion history of the Universe, independently from cosmology.

In our calculations we use  $H(z)$  measurements [45–50] ranging from  $z = 0.07$  to  $z = 1.965$ . We do not include the measurements obtained from BAO observations to avoid double counting.

### 3.4 Determination of the parameter constraints

In this work we follow a frequentist approach and minimize the standard  $\chi^2$  function to obtain the best-fit values for the parameters of our cosmological models

$$\chi^2 = (r_{\text{model}} - r_{\text{data}})^T C^{-1} (r_{\text{model}} - r_{\text{data}}), \quad (3.10)$$

where  $r_{\text{model}}$  and  $r_{\text{data}}$  are, respectively, the vectors that include the model predictions and the observed values at each redshift, and  $C$  is the covariance matrix of the data. We assume SNIa, BAO, and  $H(z)$  measurements to be statistically independent, therefore their  $\chi^2$  values can be added together. We minimize this function using the `iminuit` library<sup>1</sup> of `Python`. It is an implementation of `SEAL Minuit`, which is a minimiser developed at CERN [51].

We fit the predictions of our models for the different observables to 789 data points in total, where 740 correspond to SNIa, 16 to BAO, and 30 to  $H(z)$  measurements. For the supernova observations we have four nuisance parameters given by  $\alpha$ ,  $\beta$ ,  $M'$ , and  $\Delta M$ , which are described in Section 3.1, and two extra nuisance parameters,  $\epsilon$  and  $\delta$ , when we account for the possibility of SNIa intrinsic luminosity evolution. Specific to our models with evolving  $G$ , in addition to the cosmological parameter  $\Omega$ , we have one extra nuisance parameter,  $\tilde{a}$ , for the exponential model and between one and two parameters,  $\alpha_1$ - $\alpha_2$ , in the power series model. When considering BAO measurements we add two cosmological parameters to the analysis,  $H_0$  and  $r_d$ , as described in Section 3.2. Notice that these two parameters are completely degenerate when only SNIa and BAO data are taken into account. The introduction of measurements on  $H(z)$  breaks this degeneracy and allow us to constrain both parameters at the same time.

---

<sup>1</sup><https://pypi.org/project/iminuit/>



Model	$G(z)$ model	SN Ia lum. evo.	$\chi^2/\text{d.o.f.}$	$G_0$	$G_0^*$
0.	$\Lambda\text{CDM}$	NO	712.93/782	-	-
1.	Exponential (neg.)	NO	711.41/781	Negative	Positive
2.	Exponential (neg.)	YES	709.68/779	Negative	Positive
3.	Exponential (pos.)	NO	755.55/781	Positive	Positive
4.	Exponential (pos.)	YES	714.44/779	Positive	Positive
5.	PS (1-parameter)	NO	716.75/781	Negative	Negative
6.	PS (1-parameter)	YES	710.34/779	Negative	Negative
7.	PS (2-parameter)	NO	709.75/780	Negative	Positive
8.	PS (2-parameter)	YES	707.62/778	Negative	Positive

**Table 1.**  $\chi^2$  values over degrees of freedom for the considered models. PS refers to power series models. Exponential (pos.) refers to the exponential with positive  $\tilde{a}$  and exponential (neg.) refers to the exponential with negative  $\tilde{a}$ .

Model	$\tilde{a}$	$\Omega^a$	$\epsilon$	$\delta$	$H_0^b$	$r_d^c$	
1.	$-0.59 \pm 0.02$	$1.5 \pm 0.18$	-	-	$68.6 \pm 1.9$	$146 \pm 3.52$	
2.	$-0.61 \pm 0.03$	$1.2 \pm 0.31$	$0.12 \pm 0.14$	$0.44 \pm 1.75$	$66.4 \pm 2.53$	$147 \pm 3.57$	
3.	$0.07 \pm 0.04$	$3.59 \times 10^{-6} \pm 1.8 \times 10^{-5}$	-	-	$62.1 \pm 1.2$	$147 \pm 3.1$	
4.	$0.1 \pm 0.06$	$5.6 \times 10^{-5} \pm 23.2 \times 10^{-5}$	$0.32 \pm 0.062$	$0.42 \pm 0.20$	$62 \pm 1.46$	$148 \pm 3.59$	
Model	$\alpha_1$	$\alpha_2$	$\Omega^a$	$\epsilon$	$\delta$	$H_0^b$	$r_d^c$
5.	$-2.16 \pm 0.07$	-	$-0.68 \pm 0.09$	-	-	$67.9 \pm 1.85$	$146 \pm 3.52$
6.	$-2.31 \pm 0.20$	-	$-0.42 \pm 0.17$	$0.26 \pm 0.35$	$0.20 \pm 0.47$	$65.3 \pm 2.26$	$147 \pm 3.6$
7.	$-4.21 \pm 0.65$	$3.88 \pm 1.21$	$8.11 \pm 4.51$	-	-	$68.5 \pm 1.89$	$147 \pm 3.72$
8.	$-4.45 \pm 0.68$	$4.28 \pm 1.25$	$8.76 \pm 4.54$	$0.08 \pm 0.05$	$2.5 \pm 2.4$	$67.6 \pm 1.97$	$148 \pm 3.76$

<sup>a</sup>  $\Omega$  is negative if  $G_0^*$  is negative, <sup>b</sup>  $H_0$  has the units  $[\text{km s}^{-1} \text{Mpc}^{-1}]$ , <sup>c</sup>  $r_d$  has the units  $[\text{Mpc}]$ .

**Table 2.** Best-fit values of the cosmological parameters of the considered  $G(z)$  models.

## 4 Results and discussion

We present the  $\chi^2$  values for the tested models in Table 1 along with the flat  $\Lambda\text{CDM}$  results for comparison. The best-fit values of the cosmologically relevant parameters are given in Table 2. We do not include the nuisance parameters for SN Ia in these tables, since they do not change appreciably between the models and their small variations do not significantly contribute to the analysis. In Table 1 we can see most of the considered models are able to achieve lower  $\chi^2$  values compared to the flat  $\Lambda\text{CDM}$  case. The exceptions, model 4, the exponential with positive parameter and with SN Ia luminosity evolution, and model 5, one-parameter power series without SN Ia luminosity evolution, also have quite low  $\chi^2$  values with the exponential having comparable  $\chi^2$  to the standard model. We saw that, when considering the power series models, adding higher order terms than the second do not improve the fit, so they were not included in these tables. On the other hand, we rule out the exponential model with positive parameter without SN Ia luminosity evolution (model 3), since this model has a high  $\chi^2$ , and we do not discuss it further.

When we compare the  $\chi^2$  values of the equivalent models with and without SN Ia evolution in Table 1, we can see a slight improvement in each model when SN Ia luminosity is allowed to vary as a function of the redshift. However, since the values of the parameter  $\epsilon$  in Table 2 are compatible with zero within one sigma for models 2, 6, and 8, we can conclude



that most of our models, with the exception of the positive exponential (model 4 in Table 1), do not necessarily require SNIa luminosity evolution in order to fit the data adequately. Therefore, in Figures 1, 2 and 3, we only present models 1, 4, 5, and 7. Similarly, when we include SNIa luminosity evolution to the  $\Lambda$ CDM model for comparison, it does not change the  $\chi^2$ , with  $\epsilon$  being consistent with zero and, therefore, we do not present its results.

Turning to Table 2, we see that the results of  $H_0$  and  $r_d$  are mostly comparable between different models. We note that the best-fit values of  $H_0$  are smaller for the models that allow for SNIa luminosity evolution. Although not by much, given the error bars for  $H_0$ , models 2, 6, and 8 are still consistent with their counterparts without SNIa luminosity evolution (models 1, 5, and 7), as expected since the SNIa luminosity evolution parameters are also compatible with zero. For the exponential with positive parameter (model 4) this situation is quite different and we can confirm the effect of SNIa evolution on  $H_0$  by noting that this model predicts  $H_0 = 62.0 \pm 1.46 \text{ km s}^{-1} \text{ Mpc}^{-1}$ , which is consistent with earlier results [11]. It is evident, therefore, that adding the luminosity evolution to SNIa tends to decrease  $H_0$ , meaning that the speed of expansion implied by the cosmological data becomes lower.

There is a significant divergence in the literature between the  $H_0$  measurements given by different sources and methods (for further discussion see [11]). For instance, the Cepheid calibrated local observations provide  $H_0 = 73.48 \pm 1.66 \text{ km s}^{-1} \text{ Mpc}^{-1}$  [52]. For  $\Lambda$ CDM, Planck collaboration obtains the value  $H_0 = 67.4 \pm 0.5 \text{ km s}^{-1} \text{ Mpc}^{-1}$  [53]. Our calculations with zero or negligible SNIa evolution agree quite well with the Planck results and therefore are able to replicate a similar behaviour as the standard model, without having  $\Lambda$ . Additionally, our results are in agreement with the results given by BOSS Collaboration [54] as  $H_0 = 67.3 \pm 1.1$  using a cosmic microwave background calibrated distance scale of BAO and SNIa measurements, and the model independent estimate of Haridasu et al. [55]  $H_0 = 68.52^{+3.45}_{-0.94} \text{ km s}^{-1} \text{ Mpc}^{-1}$ , which has been obtained using Multi-Task Gaussian Process and by considering the data of SNIa, BAO, and cosmic chronometers.

Comparing the results obtained for  $r_d$  with model independent estimates, we see that, as expected, the values of  $r_d$  are not affected by the variation in SNIa luminosities. The values in Tables 2 for all the models are consistent with  $r_d = 145.61^{+2.82}_{-7.12} \text{ Mpc}$ , given by Haridasu et al. [55], as well as  $r_d = 147.4 \pm 0.7 \text{ Mpc}$ , obtained from cosmic microwave background constraints using Markov Chain Monte Carlo method by Verde et al. [56].

As discussed previously in Section 2, the actual value of  $G$  is proportional to a coefficient ( $G_0$  or  $G_\infty$ ) in Eqs. (2.8-2.9). However, these coefficients cancel out in Eq. (2.7), which we use to fit the data. For this reason, it is necessary to use additional arguments in order to determine the exact value of  $G$ . However, without making any additional assumptions, we can obtain the sign of these coefficients using

$$\Omega = \rho \frac{8\pi G_0^*}{3H_0^2}, \quad (4.1)$$

and requiring that the energy density of matter is positive, meaning that the sign of  $\Omega$  and  $G_0^*$  should be the same for any of the models, since we can compute  $G_0^*/G_0$  for the power series models and  $G_0^*/G_\infty$  for the exponential models using the best fit values. From Table 2 we see that both considered exponential models (models 1 and 4) have  $\Omega > 0$ , and that one-parameter power series (model 5) has  $\Omega < 0$  and two-parameter power series (model 7) has  $\Omega > 0$ , implying a positive  $G_0^*$  for the models 1, 4, and 7 and a negative  $G_0^*$  for the model 5. Since we calculate a positive  $G_0^*/G_0$  for the one-parameter power series and negative for the two-parameter one, while both exponential models have  $G_0^*/G_\infty = \exp(-a/\tilde{a})$  strictly

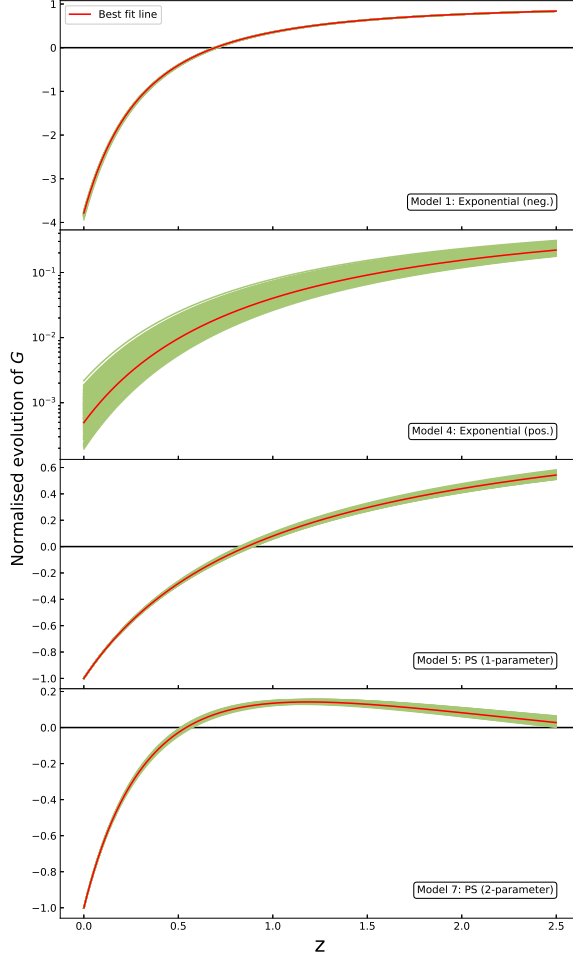
positive, we conclude that  $G_\infty$  is positive for both of the exponential models, and  $G_0$  for the power series models turns out to be negative, which means that, with the exception of the exponential model with positive parameter, all of our models predict  $G$  to be negative at the present epoch. This, of course, contradicts laboratory and Solar System experiments, but, at the phenomenological level we consider, this only implies that it is indeed necessary to have a screening mechanism to reconcile the cosmological and local scales in order to fully embrace these kind of models. However, detailing such a screening mechanism is beyond the scope of this work.

Figure 1 and 2 show the normalised evolution of  $G$ , and  $G^*$ , respectively, as a function of redshift. We present in the top panel the negative exponential model (model 1 in Table 1), the positive exponential model (model 4 in Table 1) in the second panel, and the power series models with one and two parameters (models 5 and 7 in Table 1) are shown in the third and the bottom panels, respectively. The red lines in these figures show the variation of  $-G/G_0$ , or  $G/G_\infty$ , and  $G^*/G_0^*$  as a function of redshift using the best-fit values obtained from the fit to the cosmological data sets used in this work, while errors are shown as green bands. These bands are drawn by randomly generating values for the parameters from Gaussian distributions centered at the best-fit values and width determined by the obtained standard deviations. We then select only the  $G(z)$  reconstructions whose  $\Delta\chi^2$  (compared to the best-fit  $\chi^2$ ) is smaller than one. We present the power series models in the bottom two panels of Figure 1 with the normalisation  $-G_0$ , to emphasize that  $G_0$  is found to be negative for these models. Likewise, y-axis of Figure 2 is given by  $G^*/|G_0^*|$  in order to emphasize the models with  $G_0^* < 0$ .

One interesting feature of our calculations is the appearance of two cosmological constants,  $G$  and  $G^*$ , appearing in the two Friedmann-Lemaître equations, Eqs. 2.5. In fact, this is a general feature of the variable  $G$  models. Even though we essentially modified the first equation of 2.5, and used this to derive the other, in the literature the phenomenology often adopted is modifying the gravitational constant is directly in the second equation, i.e.  $G^*$  is taken as the gravitational constant (as in [57], for instance). Then, if  $G^*$  increases sufficiently rapidly in time, it is possible to obtain an accelerated expansion in the Universe. Indeed, taking time derivative of Eq. 2.7, we obtain  $\ddot{a} = \frac{H_0^2 \Omega}{2G_0^*} \frac{d}{da}(a^{-1}G^*)$ . Therefore, if  $a^{-1}G^*$  is increasing at the late stages,  $\ddot{a}$  will be positive, implying accelerated expansion. Also, since  $G = -\frac{d}{da}(a^{-1}G^*)a^3$ ,  $G$  will become negative for the same condition. This is also evident in Figure 2, since  $G_0^*$  are positive for both of the exponential models and the two-parameter power series model, we can see that  $G^*$  never becomes negative for these models, even though  $G$  is negative for the models with accelerated expansion.

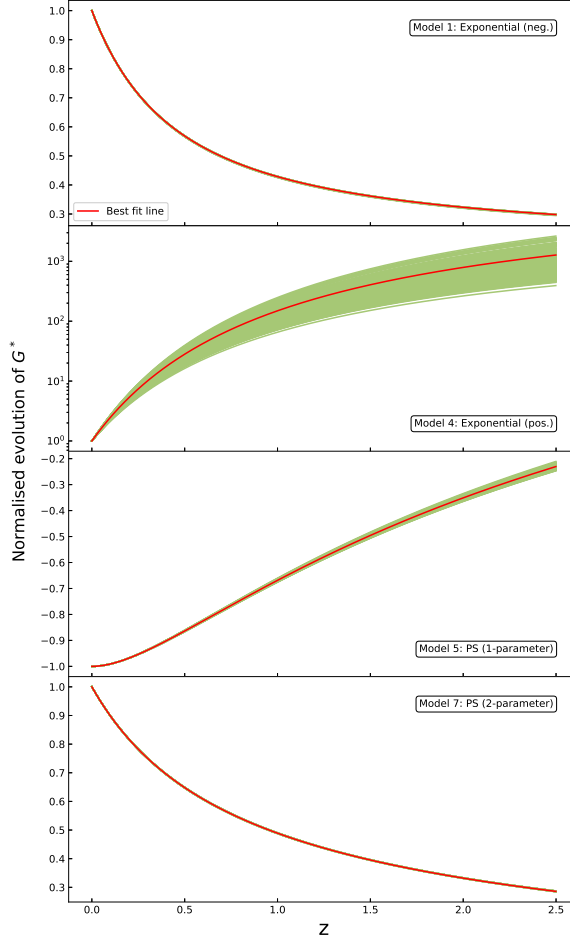
On the other hand, even though we derive our equations in a Newtonian framework, the analysis in this work would still be valid under a different theory, provided that the dynamics for the late stage expansion are analogous to Eq. 2.7. We can assume an underlying higher order theory that gives Eq. 2.7 with negative  $G$  in large scales while reducing to the usual general relativity in small scales, or high density regions. As an example of a similar situation, in conformal gravity, high level of symmetry of the Robertson-Walker metric may cause cosmological gravity to decouple from the gravitational constant of the local scales, which are, in contrast, governed by low-symmetry metrics, and spontaneous breaking of symmetry can lead to a negative  $G$  in the cosmological equations while the usual gravitational interactions are preserved locally [58].

Figure 3 displays the behaviour of the expansion rate of the Universe for the same models shown in Fig. 1 and 2 along with  $\Lambda$ CDM, in blue, for comparative purposes. Additionally,



**Figure 1.** Variation of  $G$  versus redshift for models 1, 4, 5, and 7 from Table 1 from top to bottom. The red lines represent  $-G(z)/G_0$  (for power series) or  $G(z)/G_\infty$  (for exponential) using the best-fit values for the different parameters, while the green bands encapsulate the reconstructions with  $\Delta\chi^2 < 1$  (see the text for details).

the minimum points of the y-axis in this graphs provide the transition redshift. The first panel shows the negative exponential model (model 1 in Table 1) to behave very similarly to the standard model, transitioning to the accelerated expansion at  $z_T = 0.69 \pm 0.004$ , while the power series model with one parameter (model 5 in Table 1) shows an earlier transition, at  $z_T = 0.86 \pm 0.017$ . The two-parameter power series model (model 7 in Table 1) shows almost the exact same expansion rate as  $\Lambda$ CDM after  $z \approx 0.35$  but it differs to a larger degree in higher redshifts than the one-parameter power series model. This model shows an even later transition to accelerated expansion, at  $z = 0.54 \pm 0.01$ . The presented error bars show the standard deviations of the transition redshifts of the green  $\chi^2 < 1$  bands in Figure 3. These results are consistent with  $z_T = 0.64^{+0.12}_{-0.09}$ , calculated from a model independent  $H(z)$  reconstruction [55]. Moresco et al. [45] give another model independent estimation of the transition redshift as  $z_T = 0.4 \pm 0.1$  from the five  $H(z)$  measurements they provide. While our models have larger transition redshifts than this, our results are better compatible with their other result, also provided in the same paper as  $z_T = 0.64^{+0.11}_{-0.06}$ , which takes into account



**Figure 2.** Variation of  $G^*$  versus redshift for models 1, 4, 5, and 7 from Table 1 from top to bottom. The red lines represent  $G^*(z)/|G_0^*|$  using the best-fit values for the different parameters, while the green bands encapsulate the reconstructions with  $\Delta\chi^2 < 1$  (see the text for details).

other cosmic chronometer measurements.

One interesting quality of the exponential model with positive parameter and SNIa luminosity evolution is that this model does not show late-stage acceleration, as seen by the second panel of Figure 3. Since the  $\chi^2$  for this model is also low (in Table 1), this indicates that, if SNIa intrinsic luminosity varies with cosmic time, low-redshift cosmological observations are consistent with non-accelerated dynamics, in agreement with earlier results [11].

Moreover, we can see that there is a correlation between the acceleration of different models in Figure 3 and the behaviour of  $G^*$  in Figure 2. As discussed before,  $G^*$  has to be increasing with time for the accelerated models, which corresponds to a negative  $G$  to drive the acceleration. Since these are also the models without the luminosity evolution of SNIa, this indicates that the acceleration is required by the late universe data if SNIa are assumed to have constant intrinsic luminosity.

Going forward, this study can be extended by the addition of further observations. Derivation of the equations for perturbations in the context of time-varying  $G$  would be needed for the probes sensitive to structure growth. Additionally, a relativistic extension

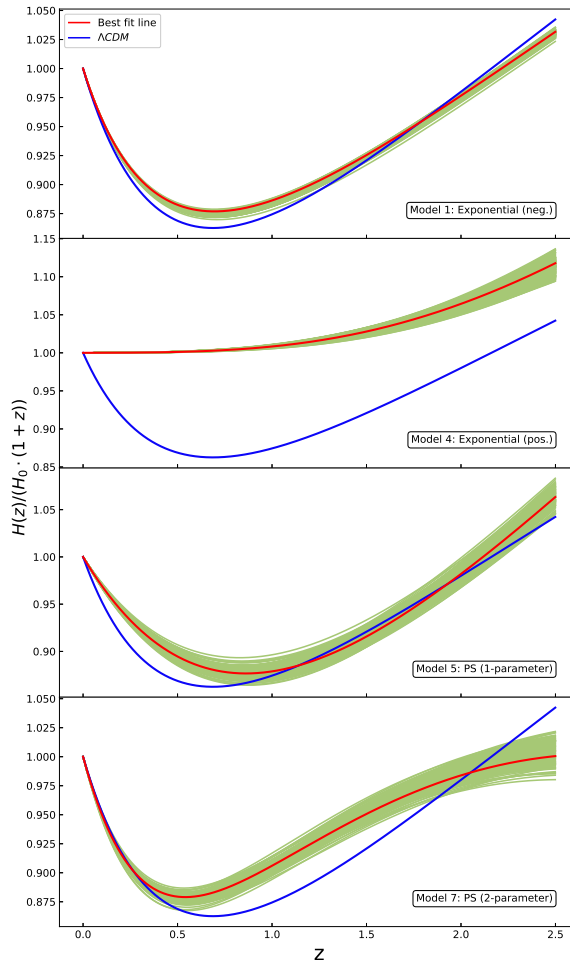


**Figure 3.** Dimensionless expansion rate of the Universe, as a function of redshift, over  $(1+z)$  for models 1, 4, 5, and 7 from Table 1 from top to bottom. The red lines represent the curve obtained with the best-fit values of the parameters, while the green bands show the reconstructions within  $\Delta\chi^2 < 1$  (see the text for details). Blue lines stand for the  $\Lambda$ CDM model.

would be required in order to consider the cosmic microwave background physics.

## 5 Conclusion

In this work we have shown that, without adding a cosmological constant, various Newtonian cosmologies with varying gravitational constant,  $G$ , are compatible with low-redshift cosmological data. A model with exponentially evolving  $G$  is shown to fit the low-redshift cosmological observations quite well when taken with a redshift dependent SNIa intrinsic luminosity. This model has positive gravitational constant,  $G$ , that decays to zero at late times, leading to a non-accelerated universe. Therefore, we see that a redshift dependence of SNIa can relieve the need for cosmic acceleration. The results for this model are also consistent with earlier analysis of  $R_h = ct$  cosmologies.

On the other hand, another exponentially varying model for  $G$  is shown to fit the data in a similar way to the flat  $\Lambda$ CDM model. This model also has an almost constant  $G$  in

high- $z$  regime, which would likely allow to match the high-redshift observations. This model does not need a modification in the SNIa luminosity but requires a negative cosmological  $G$  value in the present to propel the acceleration.

When  $G$  is expanded as a second order power series around the present epoch, we have shown that a Newtonian cosmological model can have an accelerated expansion similar to the one created by a cosmological constant with a lower  $\chi^2$  value compared to the standard model. Even though this expansion is only accurate in the very low redshifts, we see that this model is able to adequately conform to the late Universe observations.

Moreover, we show that the variable  $G$  models in general have two different gravitational parameters in the two Friedmann-Lemaître equations. We see that in an accelerated scenario, where SNIa are assumed to be standard candles, at least one of them has to be negative. Our calculations show this second gravitational parameter to be positive for both exponential models, as well as the two-parameter power series model, mentioned above.

These cosmologies only concern the late stage behaviour on large scales. Despite these constraints, we can say that they offer a viable interpretation of the low-redshift cosmological observations without explicitly requiring the introduction of a cosmological constant or dark energy.

## Acknowledgments

This work has been funded in part with support from the European Commission through Erasmus+ traineeship grant received by ETH. This publication reflects the views only of the author, and the Commission cannot be held responsible for any use which may be made of the information contained therein.

## References

- [1] A. G. Riess, A. V. Filippenko, P. Challis, A. Clocchiatti, A. Diercks, P. M. Garnavich et al., *Observational Evidence from Supernovae for an Accelerating Universe and a Cosmological Constant*, *The Astronomical Journal* **116** (1998) 1009 [[astro-ph/9805201](#)].
- [2] S. Perlmutter, G. Aldering, G. Goldhaber, R. A. Knop, P. Nugent, P. G. Castro et al., *Measurements of  $\Omega$  and  $\Lambda$  from 42 High-Redshift Supernovae*, *The Astrophysical Journal* **517** (1999) 565 [[astro-ph/9812133](#)].
- [3] A. Blanchard, *Evidence for the fifth element*, *The Astronomy and Astrophysics Review* **18** (2010) 595.
- [4] D. H. Weinberg, M. J. Mortonson, D. J. Eisenstein, C. Hirata, A. G. Riess and E. Rozo, *Observational probes of cosmic acceleration*, *Physics Reports* **530** (2013) 87 [[1201.2434](#)].
- [5] S. Weinberg, *The cosmological constant problem*, *Reviews of Modern Physics* **61** (1989) 1.
- [6] J. T. Nielsen, A. Guffanti and S. Sarkar, *Marginal evidence for cosmic acceleration from type Ia supernovae*, *Nature Sci. Rep.* **6** (2016) 35596.
- [7] H. Shariff, X. Jiao, R. Trotta and D. A. van Dyk, *Bahamas: New analysis of type Ia supernovae reveals inconsistencies with standard cosmology*, *The Astrophysical Journal* **827** (2016) 1.
- [8] D. Rubin and B. Hayden, *Is the expansion of the universe accelerating? All signs point to yes*, *The Astrophysical Journal* **833** (2016) L30.
- [9] H. I. Ringermacher and L. R. Mead, *In Defense of an Accelerating Universe: Model Insensitivity of the Hubble Diagram*, *ArXiv e-prints* (2016) [[1611.00999](#)].

- [10] I. Tutusaus, B. Lamine, A. Dupays and A. Blanchard, *Is cosmic acceleration proven by local cosmological probes?*, *A&A* **602** (2017) A73 [[1706.05036](#)].
- [11] I. Tutusaus, B. Lamine and A. Blanchard, *Model-independent cosmic acceleration and type Ia supernovae intrinsic luminosity redshift dependence*, *arXiv e-prints* (2018) arXiv:1803.06197 [[1803.06197](#)].
- [12] L. H. Dam, A. Heinesen and D. L. Wiltshire, *Apparent cosmic acceleration from type ia supernovae*, *MNRAS* **472** (2017) 835.
- [13] A. I. Lonappan, S. Kumar, Ruchika, B. R. Dinda and A. A. Sen, *Bayesian evidences for dark energy models in light of current observational data*, *Phys. Rev. D* **97** (2018) 043524 [[1707.00603](#)].
- [14] B. S. Haridasu, V. V. Luković, R. D’Agostino and N. Vittorio, *Strong evidence for an accelerating universe*, *A&A* **600** (2017) L1.
- [15] H.-N. Lin, X. Li and Y. Sang, *Local probes strongly favor  $\Lambda$ CDM against power-law and  $R_h = ct$  universe*, *Chinese Physics C* **42** (2018) 095101 [[1711.05025](#)].
- [16] V. V. Luković, B. S. Haridasu and N. Vittorio, *Cosmological Constraints from Low-Redshift Data*, *Foundations of Physics* **48** (2018) 1446 [[1801.05765](#)].
- [17] J. Colin, R. Mohayaee, M. Rameez and S. Sarkar, *Apparent cosmic acceleration due to local bulk flow*, *arXiv e-prints* (2018) [[1808.04597](#)].
- [18] P. A. M. Dirac, *The cosmological constants*, *Nature* **139** (1937) 323 EP .
- [19] P. Jordan, *Formation of the stars and development of the universe*, *Nature* **164** (1949) 637 EP .
- [20] C. Brans and R. H. Dicke, *Mach’s principle and a relativistic theory of gravitation*, *Phys. Rev.* **124** (1961) 925.
- [21] B. Bertotti, L. Iess and P. Tortora, *A test of general relativity using radio links with the cassini spacecraft*, *Nature* **425** (2003) 374 EP .
- [22] A. Joyce, B. Jain, J. Khoury and M. Trodden, *Beyond the cosmological standard model*, *Physics Reports* **568** (2015) 1 .
- [23] J. Sultana, *Comment on ”varying-g cosmology with type ia supernovae”*, *American Journal of Physics* **83** (2015) 570 [<https://doi.org/10.1119/1.4907266>].
- [24] J. D. Barrow, *Varying constants*, *Philosophical Transactions of the Royal Society A: Mathematical, Physical and Engineering Sciences* **363** (2005) 1 .
- [25] J. D. Barrow, *Time-varying G*, *Monthly Notices of the Royal Astronomical Society* **282** (1996) 1397 [<http://oup.prod.sis.lan/mnras/article-pdf/282/4/1397/18540387/282-4-1397.pdf>].
- [26] M. Milgrom, *A modification of the Newtonian dynamics as a possible alternative to the hidden mass hypothesis*, *The Astrophysical Journal* **270** (1983) 365.
- [27] J. P. Vinti, *Classical Solution of the Two-Body Problem If the Gravitational Constant Diminishes Inversely with the Age of the Universe*, *Monthly Notices of the Royal Astronomical Society* **169** (1974) 417 [<http://oup.prod.sis.lan/mnras/article-pdf/169/3/417/9402898/mnras169-0417.pdf>].
- [28] C. Duval, G. Gibbons and P. Horváthy, *Celestial mechanics, conformal structures, and gravitational waves*, *Phys. Rev. D* **43** (1991) 3907.
- [29] F. Melia, *The cosmic horizon*, *Monthly Notices of the Royal Astronomical Society* **382** (2007) 1917 [<http://oup.prod.sis.lan/mnras/article-pdf/382/4/1917/3961269/mnras0382-1917.pdf>].



- [30] F. Melia and A. S. H. Shevchuk, *The  $R_h=ct$  universe*, *Monthly Notices of the Royal Astronomical Society* **419** (2012) 2579 [<http://oup.prod.sis.lan/mnras/article-pdf/419/3/2579/18718282/mnras0419-2579.pdf>].
- [31] I. Tutusaus, B. Lamine, A. Blanchard, A. Dupays, Y. Zolnierowski, J. Cohen-Tanugi et al., *Power law cosmology model comparison with cmb scale information*, *Phys. Rev. D* **94** (2016) 103511.
- [32] M. V. John,  *$R_h=ct$  and the eternal coasting cosmological model*, *Monthly Notices of the Royal Astronomical Society: Letters* **484** (2019) L35 [<http://oup.prod.sis.lan/mnrasl/article-pdf/484/1/L35/27519856/sly243.pdf>].
- [33] K. Koyama and J. Sakstein, *Astrophysical Probes of the Vainshtein Mechanism: Stars and Galaxies*, *Phys. Rev.* **D91** (2015) 124066 [[1502.06872](#)].
- [34] Y. Zolnierowski and A. Blanchard, *Dark energy dependent test of general relativity at cosmological scales*, *Phys. Rev. D* **91** (2015) 083536.
- [35] M. Betoule, R. Kessler, J. Guy, J. Mosher, D. Hardin, R. Biswas et al., *Improved cosmological constraints from a joint analysis of the SDSS-II and SNLS supernova samples*, *A & A* **568** (2014) A22 [[1401.4064](#)].
- [36] L. Verde, J. L. Bernal, A. F. Heavens and R. Jimenez, *The length of the low-redshift standard ruler*, *Monthly Notices of the Royal Astronomical Society* **467** (2017) 731 [<http://oup.prod.sis.lan/mnras/article-pdf/467/1/731/10493711/stx116.pdf>].
- [37] F. Beutler, C. Blake, M. Colless, D. H. Jones, L. Staveley-Smith, L. Campbell et al., *The 6dF Galaxy Survey: baryon acoustic oscillations and the local Hubble constant*, *Mon. Notices Royal Astron. Soc* **416** (2011) 3017 [[1106.3366](#)].
- [38] A. J. Ross, L. Samushia, C. Howlett, W. J. Percival, A. Burden and M. Manera, *The clustering of the SDSS DR7 main Galaxy sample - I. A 4 per cent distance measure at  $z = 0.15$* , *MNRAS* **449** (2015) 835 [[1409.3242](#)].
- [39] S. Alam, M. Ata, S. Bailey, F. Beutler, D. Bizyaev, J. A. Blazek et al., *The clustering of galaxies in the completed SDSS-III Baryon Oscillation Spectroscopic Survey: cosmological analysis of the DR12 galaxy sample*, *Mon. Notices Royal Astron. Soc* **470** (2017) 2617 [[1607.03155](#)].
- [40] H. Gil-Marín, J. Guy, P. Zarrouk, E. Burtin, C.-H. Chuang, W. J. Percival et al., *The clustering of the SDSS-IV extended Baryon Oscillation Spectroscopic Survey DR14 quasar sample: structure growth rate measurement from the anisotropic quasar power spectrum in the redshift range  $0.8 < z < 2.2$* , *Mon. Notices Royal Astron. Soc* **477** (2018) 1604 [[1801.02689](#)].
- [41] J. E. Bautista, N. G. Busca, J. Guy, J. Rich, M. Blomqvist, H. du Mas des Bourboux et al., *Measurement of baryon acoustic oscillation correlations at  $z = 2.3$  with SDSS DR12 Ly $\alpha$ -Forests*, *A & A* **603** (2017) A12.
- [42] H. du Mas des Bourboux, J.-M. Le Goff, M. Blomqvist, N. G. Busca, J. Guy, J. Rich et al., *Baryon acoustic oscillations from the complete SDSS-III Ly $\alpha$ -quasar cross-correlation function at  $z = 2.4$* , *A & A* **608** (2017) A130 [[1708.02225](#)].
- [43] B. A. Bassett and N. Afshordi, *Non-Gaussian Posteriors arising from Marginal Detections*, *arXiv e-prints* (2010) arXiv:1005.1664 [[1005.1664](#)].
- [44] R. Jimenez and A. Loeb, *Constraining cosmological parameters based on relative galaxy ages*, *The Astrophysical Journal* **573** (2002) 37.
- [45] M. Moresco, L. Pozzetti, A. Cimatti, R. Jimenez, C. Maraston, L. Verde et al., *A 6% measurement of the Hubble parameter at  $z \sim 0.45$ : direct evidence of the epoch of cosmic re-acceleration*, *JCAP* **1605** (2016) 014 [[1601.01701](#)].

- [46] M. Moresco, *Raising the bar: new constraints on the Hubble parameter with cosmic chronometers at  $z \sim 2$* , *Monthly Notices of the Royal Astronomical Society: Letters* **450** (2015) L16 [<http://oup.prod.sis.lan/mnrasl/article-pdf/450/1/L16/3083577/slv037.pdf>].
- [47] M. Moresco, A. Cimatti, R. Jimenez, L. Pozzetti, G. Zamorani, M. Bolzonella et al., *Improved constraints on the expansion rate of the universe up to  $z \sim 1.1$  from the spectroscopic evolution of cosmic chronometers*, *Journal of Cosmology and Astroparticle Physics* **2012** (2012) 006.
- [48] J. Simon, L. Verde and R. Jimenez, *Constraints on the redshift dependence of the dark energy potential*, *Phys. Rev. D* **71** (2005) 123001.
- [49] D. Stern, R. Jimenez, L. Verde, S. A. Stanford and M. Kamionkowski, *COSMIC CHRONOMETERS: CONSTRAINING THE EQUATION OF STATE OF DARK ENERGY. II. a SPECTROSCOPIC CATALOG OF RED GALAXIES IN GALAXY CLUSTERS*, *The Astrophysical Journal Supplement Series* **188** (2010) 280.
- [50] C. Zhang, H. Zhang, S. Yuan, S. Liu, T.-J. Zhang and Y.-C. Sun, *Four new observational  $H(z)$  data from luminous red galaxies in the sloan digital sky survey data release seven*, *Research in Astronomy and Astrophysics* **14** (2014) 1221.
- [51] F. James and M. Roos, *Minuit - a system for function minimization and analysis of the parameter errors and correlations*, *Computer Physics Communications* **10** (1975) 343.
- [52] A. G. Riess, S. Casertano, W. Yuan, L. Macri, J. Anderson, J. W. MacKenty et al., *New parallaxes of galactic cepheids from spatially scanning the hubble space telescope: Implications for the hubble constant*, *The Astrophysical Journal* **855** (2018) 136.
- [53] Planck Collaboration, N. Aghanim, Y. Akrami, M. Ashdown, J. Aumont, C. Baccigalupi et al., *Planck 2018 results. VI. Cosmological parameters*, *arXiv e-prints* (2018) arXiv:1807.06209 [[1807.06209](https://arxiv.org/abs/1807.06209)].
- [54] BOSS collaboration, *Cosmological implications of baryon acoustic oscillation measurements*, *Phys. Rev. D* **92** (2015) 123516.
- [55] B. S. Haridasu, V. V. Luković, M. Moresco and N. Vittorio, *An improved model-independent assessment of the late-time cosmic expansion*, *JCAP* **1810** (2018) 015 [[1805.03595](https://arxiv.org/abs/1805.03595)].
- [56] L. Verde, E. Bellini, C. Pigozzo, A. F. Heavens and R. Jimenez, *Early cosmology constrained*, *Journal of Cosmology and Astroparticle Physics* **2017** (2017) 023.
- [57] O. Zahn and M. Zaldarriaga, *Probing the friedmann equation during recombination with future cosmic microwave background experiments*, *Phys. Rev. D* **67** (2003) 063002.
- [58] P. D. Mannheim, *Attractive and repulsive gravity.*, *Foundations of Physics* **30** (2000) 709 [[gr-qc/0001011](https://arxiv.org/abs/gr-qc/0001011)].